ELSEVIER

Calcium-mediated fulvene couplings. 3. Reductive coupling of guaiazulene with activated calcium to give a mixture of 8,6′ and 8,8′ (diguaiazulenide)calcium isomers. Thermal rearrangement of the 8,6′ isomer to the 8,8′ isomer and X-ray crystal structure of the 8,8′ isomer

Piet-Jan Sinnema, Pamela J. Shapiro *, Britta Höhn, Brendan Twamley

Department of Chemistry, University of Idaho, Moscow, ID 83844-2343, USA

Abstract

The reductive coupling of guaiazulene with activated calcium in THF at 30–35 °C affords a 60:40 mixture of two isomers, 8,8′-(**1**) and 8,6′-(**2**) (diguaiazulenide)bis(tetrahydrofuran)calcium, respectively, in nearly quantitative yield. The isomers were separated and purified by recrystallization. The X-ray crystal structure of **1** is reported. A modest dependence of the isomer ratio on the reaction temperature was noticed. At lower temperature (9 °C) the 8,6′ isomer, **2**, is favored slightly, and at higher temperature (67 °C) selectivity for the 8,8′ isomer, **1**, is slightly enhanced. Thermolyses of each isomer revealed that **1** is the thermodynamically preferred isomer.

1. Introduction

The reductive coupling of fulvenes with metals such as Mg [1], Ca [2], Sr [2a], Sm and Yb [3], or with low valent metal species like [MCl$_2$] (M = Ti, Zr, Hf) [4] offers an elegant single-step procedure for synthesizing *ansa*-metallocenes. The stereoselective synthesis of C_2-symmetric *ansa*-metallocenes using this fulvene reductive coupling chemistry has been demonstrated successfully in a handful of cases; however, the applicability of this method to the synthesis of chiral *ansa*-metallocenes is still far from general. Eisch et al. found that in situ generated ZrCl$_2$ couples unsymmetrically substituted 6-aryl fulvenes with increasing selectivity for the *rac ansa*-zirconocene isomer as the size of the aryl group is increased from phenyl to 1-naphthyl to 9-anthryl [4]. Activated calcium, on the other hand, exhibits little to no selectivity for the *rac* over the *meso ansa*-calcocene isomer when bulky substituents such as 1-naphthyl, *t*-butyl, and 3,5-di-*t*-butylphenyl groups are present on

the fulvene [2h]. The differences in the stereoselectivities of the homogeneous vs. the heterogeneous reductants can perhaps be attributed to the degree with which the fulvene substrates are able to pre-organize on the reducing species prior to their coupling [5].

Polycyclic fulvenes, in which the *exo* double bond of the fulvene is part of an annulated ring system, are the only substrates that consistently afford *rac ansa*-metallocenes with high selectivity, even when coupled in a heterogeneous manner by activated metals. For example, Brintzinger and coworkers obtained only the *rac*-isomer of [8,8′-diguaiazulenide]titanium dichloride, albeit in low yield (10%), upon coupling guaiazulene with Mg/CCl$_4$ and transferring the resulting ligand to titanium [6]. Erker and coworkers coupled 4,4-dimethyl-7-phenyl-bicyclo[4,3,0]cyclonona-1,3,8-triene stereoselectively with activated calcium, isolated the calcium-free ligand and used its dilithium salt to prepare *rac*-[7,7′-bis(7-phenyl-4,4-dimethyl-4,5,6,7-tetrahydroindenylene)]zirconium dichloride [7]. Recently, Schumann and coworkers reported the stereospecific formation of C_2-symmetric *ansa*-calcocene and *ansa*-lanthanocene com-

* Corresponding author.

plexes from the reductive coupling of acenaphthylene with the activated metals [3c,8]. Transmetallation of the resulting bridged ligand framework from ytterbium to zirconium resulted in cleavage of the bridge [9]. We have encountered a similar problem in attempting to transfer the same ligand framework from calcium to chromium [10].

With the goal of generating chiral *ansa*-calcocene compounds as precursors to chiral metallocene complexes of the early transition metals, we reexamined the guaiazulene ligand as a substrate for this reductive coupling chemistry. The bicyclic structure of guaiazulene, the apparent *rac*-selectivity of its coupling by Mg, and the commercial availability and low cost of the fulvene made it an attractive candidate for the synthesis of a *rac ansa*-calcocene complex. Besides obtaining the expected C_2-symmetric *ansa*-calcocene isomer, [8,8′-diguaiazulenide]calcium (**1**), from this reaction, we obtained a comparable amount of another asymmetric calcocene species, [8,6′-diguaiazulenide]calcium (**2**). Herein we describe the synthesis, separation and structural characterization of these two calcocene isomers. We also report the first example of the thermal isomerization of an *ansa*-metallocene species via the cleavage and reformation of the interannular bridge.

2. Results

2.1. Reaction of guaiazulene with activated calcium

When a mixture of guaiazulene and $HgCl_2$-activated calcium chips in THF is heated at 30–35 °C for several hours (5–12 h depending on the quality of the activated calcium) the intense blue color of the guaiazulene disappears, signaling completion of the reaction. The *ansa*-calcocene product is isolated in nearly quantitative yield (94%) as an off-white powder.

In such a reaction, two crops of calcocene product were isolated by crystallization from the resulting gray, turbid mixture after removal of excess, unreacted calcium. The ^{1}H-NMR spectrum of the first crop (49.5% yield) in THF-d_8 revealed two species in a 90:10 ratio. The ^{1}H-NMR spectrum of the second crop (44.5% yield) revealed the same two species in a 26:74 ratio. This gives an overall ratio of 60:40 for the two isomers. The separation and purification of each isomer was achieved by virtue of their different solubilities in THF and DME. Recrystallization of the first crop from THF yielded the major component as a single pure compound whose structure was established as *rac*-[8,8′-diguaiazulenide]Ca(THF)$_2$ (**1**) by NMR spectroscopy and by single-crystal X-ray diffraction (vide infra). The ^{1}H-NMR spectrum of **1** is very similar to that reported for *rac*-[8,8′-diguaiazulenide]TiCl$_2$ [6]. Four doublets at δ 5.69 ($^3J_{HH} = 6.73$ Hz), 5.63

($^3J_{HH} = 3.35$ Hz), 5.57 ($^3J_{HH} = 3.35$ Hz) and 5.52 ($^3J_{HH} = 6.73$ Hz) are observed for the olefinic protons of the five- and seven-membered rings of the guaiazulenide moieties. The protons of the bridgehead carbon atoms appear as one singlet at δ 4.13. The bridgehead carbons show aliphatic features in the ^{13}C-NMR spectrum (δ 44.91, $^1J_{CH} = 129.4$ Hz) consistent with their sp^3 hybridization. The two pairs of methyl groups appear as singlets at δ 2.14 and 1.97. The methine protons of the isopropyl groups appear as a heptet (δ 2.51, $^3J_{HH} = 6.74$ Hz), and the methyl protons give rise to two doublets (δ 1.00 and 0.86, $^3J_{HH} = 6.74$ Hz).

Recrystallization of the second crop from DME afforded the major component of that fraction, the second isomer **2**, in 95% purity. The identity of this isomer as [8,6′-diguaiazulenide]Ca(DME) was established by a combination of one and two dimensional NMR techniques (^{1}H, ^{13}C, COSY, HMQC, HMBC). A preliminary X-ray crystal structure of the compound confirmed our assignment [11]. The structure also revealed that the guaiazulene rings in **2** are in a *meso*-like arrangement, as opposed to the *rac* arrangement in **1**. In other words, the calcium is bound to different faces of the two guaiazulene ring systems such that the isopropyl and methyl substituents on one ring system are oriented in more or less the same direction as the corresponding substituents on the opposite ring system (see Scheme 1 below). Unfortunately, the quality of the data is not adequate for publication of the structure at this time. The ^{1}H-NMR spectrum of **2** (in THF-d_8) [12] is more complex than that of **1** since **2** has lower symmetry. Six resonances instead of four are found in the olefinic region: three singlets at δ 6.12 (1H), δ 5.46 (2H), and δ 5.44 ppm (2H), two mutually coupled doublets at δ 5.67 and 5.62, and a doublet of doublets at δ 5.21 ($J_{HH} = 8.58$ and 1.13 Hz, 1H). The protons on the bridgehead carbons appear as two separate resonances at δ 3.39 (d, $J_{HH} = 2.0$ Hz) and δ 3.07 (dd, $J_{HH} = 2.0$ and 8.58 Hz). The latter is coupled with the proton resonating at δ 5.21. Due to the absence of symmetry in the molecule, the methyl substituents on the ligand give rise to four singlets and the isopropyl groups give rise to two methine heptets and four doublet methyl resonances. There are twice as many ^{13}C-NMR resonances for the ligand framework in **2** than in **1**.

2.2. Temperature dependence of ansa-calcocene isomer ratio and thermal conversion of 2 to 1

The combined *ansa*-calcocene product obtained from the coupling of guaiazulene at 30–35 °C revealed a 60:40 ratio of **1**:**2**. When the calcium-mediated reductive coupling was performed at 9 °C, a 46:54 ratio of **1**:**2** was obtained instead. Performing the reaction in refluxing THF (ca. 67 °C) afforded a 58:42 ratio of isomers. In order to determine if the slight preponder-

Scheme 1.
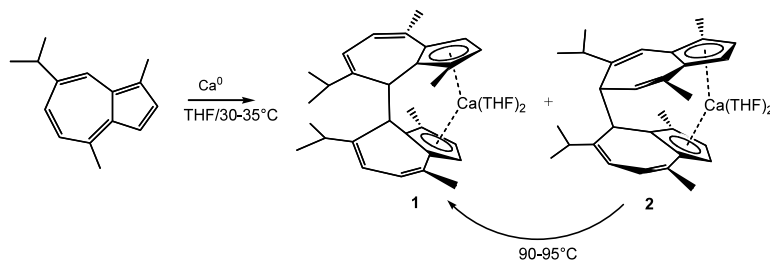
ance of **1** at the higher temperatures might be due to the isomerization of **2** to **1**, the thermolyses of these species were examined. The thermolyses of the pure isomers in THF-d_8 were monitored by ^{1}H-NMR spectroscopy. Although no isomerization of **2** to **1** was observed over a 1-week period at room temperature, heating the sample to 90–95 °C did result in the slow conversion of isomer **2** completely to isomer **1** over 36 h. Some decomposition of the complex was noted from the appearance of free guaiazulene (8%). The reverse reaction, conversion of **1** to **2**, was not observed after heating a solution of **1** in THF-d_8 at 90–95 °C for 36 h, although a small amount of free guaiazulene ($\sim$3%) formed.

2.3. Molecular structure of [8,8'-diguaiazulenide]Ca(THF)$_2$ (**1**)

Crystallographic data for isomer **1** are listed in Table 1. Selected geometric data are given in Table 2. As can be seen from the ORTEP drawing in Fig. 1, the calcium atom is in a pseudo-tetrahedral coordination environment with both five-membered rings of the ligand bound η^5 to the calcium center. The centroid-calcium-centroid angle of 120.2°, the O(1)–Ca–O(2) angle of 84.30(9)°, the average Ca–O bond length of 2.389(6) Å and the average Ca-centroid distance of 2.412(9) Å, are all within the range found for these parameters in related *ansa*-calcocene complexes [2b,2d,2e,2f,2g,2h]. The opposite orientation of the fused guaiazulenide ligands and the conformations of their isopropyl substituents confer a C_2-symmetry to the structure. The π electrons in the five-membered rings are fully delocalized with an average C–C bond length 1.415 Å and bond length differences of less than 0.016 Å. By contrast, the seven-membered rings contain localized single and double C–C bonds, with double bond distances of 1.345–1.352 Å and single bond distances of 1.447–1.523 Å. The bond distance between the bridgehead carbon atoms C(7) and C(22), 1.577(4) Å, is similar to that found for the *ansa*-titanocene system and is somewhat longer than other single C–C bonds in the structure (ca. 1.52 Å). It is also somewhat longer than the corresponding C–C bridges in less rigid ethano-bridged *ansa*-calcocene complexes (ca. 1.52 Å) [2] and comparable in length to the bridgehead bond in the two independent molecules in

Table 1
Crystallographic data for **1** (0.5 THF)

Empirical formula	$C_{40}H_{56}CaO_{2.50}$
Formula weight	616.93
Crystal system	Monoclinic
Space group	$P2_1/c$
a (Å)	15.3005(17)
b (Å)	17.450(2)
c (Å)	14.2911(16)
α (°)	90
β (°)	96.39(2)
γ (°)	90
V (Å^3)	3792.19(8)
Z	4
Temperature (K)	203(2)
λ (Å)	0.71073
ρ_{calc} (Mg m^{-3})	1.081
μ (mm^{-1})	0.197
$F_{(0\,0\,0)}$	1344
Crystal size (mm^3)	$0.55 \times 0.40 \times 0.25$
θ Range (°)	1.85–25.00
Index ranges	$-18 \leq h \leq 14,\ -20 \leq k \leq 20,$ $-11 \leq l \leq 16$
Number of reflections collected	27253
Number of independent reflections	6665 [$R_{int} = 0.0368$]
Data/restraints/parameters	6665/0/423
Goodness-of-fit on F^2	1.097
$R(F_o)\ [I > 2\sigma(I)]$	0.0639
$wR(F_o^2)\ [I > 2\sigma(I)]$	0.1863

the unit cell of the 3,3'-(diacenapthylenide)calcium complex (avg. 1.57 Å) [8].

3. Discussion and conclusions

Scheme 1 provides a summary of our results from the calcium-mediated reductive coupling of guaiazulene and the subsequent thermolysis of the 6,8' coupling product, isomer **2**, to isomerize it to the 8,8' coupling product, isomer **1**.

Although there is precedent for both the 6,8' and 8,8' coupling products from the reaction of guaiazulene and azulene with Mg(0) [6] and Fe(0) [13], respectively, this is the first time that both isomers have been detected together from the same reductive coupling reaction [14]. The kinetic preference for either isomer was small at all

Table 2
Selected bond distances (Å) and angles (°) for **1**

Ca(1)–O(2)	2.384(2)	C(5)–C(11)	1.461(4)
Ca(1)–O(1)	2.393(2)	C(17)–C(21)	1.409(4)
Ca–cent(C2–C6)	2.406(6)	C(17)–C(18)	1.415(4)
Ca–cent(C17–21)	2.419(7)	C(18)–C(19)	1.402(4)
Ca(1)–C(18)	2.668(3)	C(19)–C(20)	1.427(4)
Ca(1)–C(17)	2.675(3)	C(20)–C(21)	1.427(4)
Ca(1)–C(3)	2.680(3)	C(7)–C(22)	1.577(4)
Ca(1)–C(4)	2.682(3)	C(6)–C(7)	1.508(4)
Ca(1)–C(2)	2.683(3)	C(5)–C(11)	1.461(4)
Ca(1)–C(6)	2.692(3)	C(7)–C(8)	1.522(4)
Ca(1)–C(19)	2.702(3)	C(8)–C(9)	1.348(4)
Ca(1)–C(21)	2.707(3)	C(9)–C(10)	1.459(4)
Ca(1)–C(5)	2.713(3)	C(10)–C(11)	1.352(4)
Ca(1)–C(20)	2.758(3)	C(20)–C(26)	1.455(4)
C(2)–C(3)	1.417(4)	C(21)–C(22)	1.506(4)
C(3)–C(4)	1.400(4)	C(22)–C(23)	1.523(4)
C(4)–C(5)	1.418(4)	C(23)–C(24)	1.346(4)
C(5)–C(6)	1.423(4)	C(24)–C(25)	1.457(4)
C(2)–C(6)	1.409(4)	C(25)–C(26)	1.347(4)
O(2)–Ca(1)–O(1)	84.31(8)	C(9)–C(8)–C(7)	121.0(3)
C(6)–C(7)–C(8)	110.1(2)	C(8)–C(9)–C(10)	129.1(3)
C(6)–C(7)–C(22)	115.3(2)	C(11)–C(10)–C(9)	129.0(3)
C(10)–C(11)–C(5)	122.8(3)	C(8)–C(7)–C(22)	108.8(2)
C(21)–C(22)–C(23)	110.6(2)	C(23)–C(22)–C(7)	108.8(2)
C(21)–C(22)–C(7)	115.9(2)	C(25)–C(26)–C(20)	123.2(3)
cent–Ca–cent [a]	120.2	Cp < Cp [b]	59.3

[a] cent, Center of five membered rings.
[b] Cp, five membered rings.

Fig. 2. Drawings of guaiazulene showing carbon atom numbering and carbon π-orbital coefficients of the LUMO from PM3 calculations.

in the LUMO of guaiazulene are at carbon positions 8, 4, and 6 (Fig. 2) with absolute values of the orbital coefficients of 0.49, 0.29, and 0.46, respectively. The orbital density characteristics are consistent with our detection of both 8,8′ and 6,8′ ring coupling products. The failure of carbon 4 to participate in bridge formation is probably due to a combination of steric interference from the methyl substituent at that position as well as the lower orbital density coefficient at that position. It is noteworthy that no unbridged calcocene products that could arise from hydrogen abstraction from the methyl substituent at carbon 4 were observed, especially since this side reaction did occur in the coupling of Erker's bicyclic fulvene, 4,4-dimethyl-7-phenyl-bicyclo[4,3,0]cyclonona-1,3,8-triene, with calcium [2c].

Two types of rearrangements must occur in order for **2** to isomerize to **1**. Besides cleavage of the 6,8′ bridge and reformation of an 8,8′ bridge, the calcium also must switch faces on one of its guaiazulenide ligands in order to achieve a C_2-symmetric arrangement. Although bridge cleavage was observed previously in attempts to transfer the 3,3′-diacenaphthylenide ligand from ytterbium and calcium to transition metals [9,10], to our knowledge, this is the first report of the formation of a new bridge following bridge cleavage in an *ansa*-metallocene complex.

In summary, comparable amounts of the expected 8,8′ coupled *rac* isomers **1** and the 6,8′ coupled *meso*-like isomer **2** are formed in the reductive coupling of guaiazulene by calcium. Despite the poor regioselectivity of the coupling reaction, complete conversion of **1** to **2**

three reaction temperatures (−9 °C, 30–35 °C, refluxing THF). In terms of stereochemistry, isomer **1** is *rac* and isomer **2** can be regarded as *meso*-like. Therefore, the stereoselectivity of the coupling by calcium is poor, as observed previously. The position of the bridge is specific to each stereoisomer, however. In order to understand the location of the bridge in each isomer, it is instructive to consider the π orbital characteristics of the LUMO of guaiazulene since the orbital density on the carbons of the cycloheptatriene ring in the LUMO will influence the regioselectivity of the coupling. Semi-empirical calculations at the PM3 level confirm that the bulk of the π orbital density of the seven-membered ring
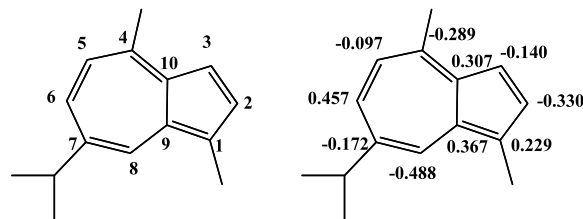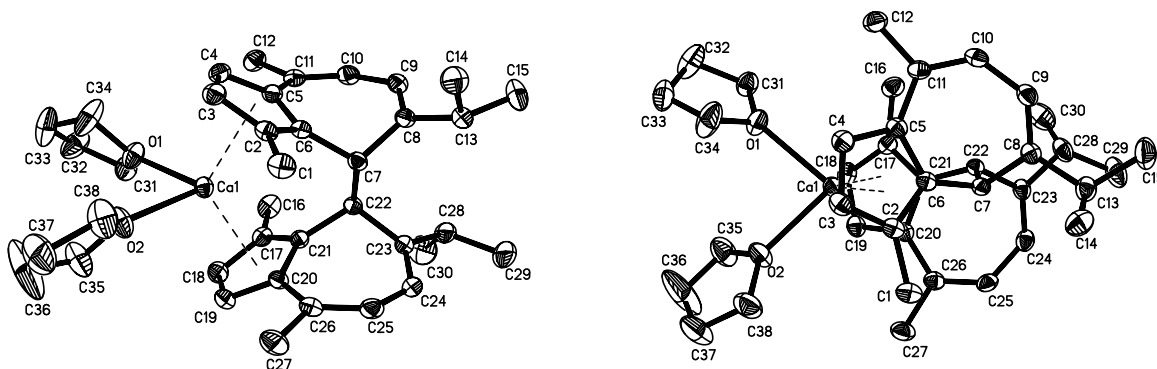

Fig. 1. Top and side views of the molecular structure of **1** (30% ellipsoids).

can be achieved thermally and involves *ansa*-bridge cleavage and reformation. Such isomerization is significant for the application of this fulvene coupling methodology to the synthesis of C_2-symmetric *ansa*-metallocenes. Unfortunately, the tendency of the bridge in the *ansa*-diguaiazulenide ligand framework to undergo cleavage also interferes with its transfer from calcium to other metals. Our efforts to transfer the 8,8′-diguaiazulenide ligand from calcium to either chromium or zirconium have resulted in the isolation of only free guaiazulene. We suspect that the reversibility of this guaiazulene dimerization is associated with the high stability of the aromatic monomeric species. Future work will focus on modifying the diguaiazulenide ligand framework while it is on calcium in order to discourage its cleavage to monomers during transmetallation.

4. Experimental

All manipulations were performed under an argon or nitrogen atmosphere using Schlenk glassware, glovebox (Braun MB 130-BG) or vacuum line techniques. HPLC grade THF and pentane were dried by passage over alumina and then stored over sodium/benzophenone in vacuum line pots. DME was freshly distilled from sodium/benzophenone and stored over sodium/benzophenone in a vacuum line pot. Argon was purified by passage over oxytower BASF catalyst (Aldrich) and 4 A molecular sieves. DMSO-d_6 and THF-d_8 were dried over 4 A molecular sieves and stored in the glovebox. Granulated calcium was activated by stirring it overnight in THF in the presence of 1 mol.% of $HgCl_2$ as described by Rieckhoff et al. [2a]. Guaiazulene was purchased from Aldrich and used without further purification. ^{1}H and ^{13}C-NMR spectra were recorded on Bruker AMX 300 (300 MHz, ^{1}H; 75 MHz, ^{13}C) or Bruker AVANCE 500 (500 MHz, ^{1}H; 125 MHz, ^{13}C) spectrometers. The chemical shifts are reported relative to TMS and the resonances of the residual protons and ^{13}C carbons in THF-d_8 were used as references. The LUMO orbital densities for guaiazulene were determined from semi-empirical calculations at the PM3 level that were performed with the software package MAC-SPARTAN PLUS (© 1996, Wavefunction Inc., Irvine CA).

4.1. Reaction of activated calcium with guaiazulene: isolation of [8,8′-diguaiazulenide]Ca(THF)$_2$ (1) and [8,6′-diguaiazulenide]Ca(THF)$_2$ (2)

THF (120 ml) was condensed onto a mixture of 16.0 g (80.7 mmol) of guaiazulene and 2.54 g (63.4 mmol) of activated calcium at −196 °C and the mixture was warmed to room temperature. The intense dark blue reaction mixture was stirred overnight at 30–35 °C, producing a gray, turbid mixture when the reaction was

complete. The remaining fine calcium particles were allowed to settle from the mixture for 24 h. The solution was decanted from the particles and passed through a filter, at which point the product started to crystallize. The filtrate was further concentrated in vacuo and cooled with an ice-bath to promote further precipitation of the product. The mother liquor was removed by filtration and the product was dried under vacuum, affording 11.62 g of an off-white product. The ^{1}H-NMR spectrum showed the product to be a mixture of [8,8′-diguaiazulenide]Ca(THF)$_2$ (90%) and [8,6′-diguaiazulenide]Ca(THF)$_2$ (10%). The mother liquor was concentrated and cooled at −30 °C to afford a second crop of product (10.45 g). The ^{1}H-NMR spectrum showed this product to be a mixture of [8,8′-diguaiazulenide]-Ca(THF)$_2$ (26%) and [8,6′-diguaiazulenide]Ca(THF)$_2$ (74%). Total isolated coupling products 22.07 g (38.0 mmol, 94%, based on guaiazulene). The overall ratio of **1**:**2** was 60:40. An analytically pure sample of **1** was obtained by recrystallization of the first crop from THF.

An analytically pure [8,6′-diguaiazulenide]Ca(DME) (**2DME**) was obtained by stirring a 3.45 g (5.94 mmol) sample of the second crop in 50 ml of DME. The DME was removed in vacuum and fresh DME (50 ml) was distilled into the vessel. Extraction yielded an almost white powder which was washed with pentane (50 ml) and dried under vacuum (Yield: 2.10 g, 73%).

A reaction performed in a thermostated bath at 9 °C with 10.5 g (52.9 mmol) of guaiazulene and 1.89 g (47.2 mmol) of activated calcium in 100 ml of THF (16 h stirring) yielded 15.12 g (98%) of product. The ^{1}H-NMR spectrum of the product showed it to be a mixture of 46% **1** and 54% **2THF**.

A reaction performed overnight in refluxing THF between 4.80 g (24.2 mmol) of guaiazulene and 1.12 g (27.9 mmol) of activated calcium in 80 ml of THF gave 6.63 g (11.4 mmol, 94%) of product. A ^{1}H-NMR spectrum of the product showed it to be a mixture of 58% of **1** and 42% of **2THF**.

The proton and carbon signals in the NMR spectra of **1** are labeled according to the numbering scheme given to its molecular structure in Fig. 1.

4.1.1. NMR data for 1

^{1}H-NMR (500.13 MHz, THF-d_8): δ 5.69 (d, $^3J_{HH}$ = 6.73 Hz, 2H, H(10/25)); 5.63 (d, $^3J_{HH}$ = 3.35 Hz, 2H, H(4/19)); 5.57 (d, $^3J_{HH}$ = 3.35 Hz, 2H, H(3/18)); 5.52 (d, $^3J_{HH}$ = 6.73 Hz, 2H, H(9/24)); 4.13 (s, 2H, H(7/22); 3.58 (m, 8H, THF); 2.51 (hept, $^3J_{HH}$ = 6.74 Hz, 2H, H(13/28); 2.14 (s, 6H, H(12/27)); 1.97 (s, 6H, H(1/16)); 1.73 (m, 8H, THF); 1.00, 0.86 (2d, $^3J_{HH}$ = 6.74 Hz, 6.74 Hz, 6H+6H, Hs at C(14/15/29/30)). ^{13}C-NMR (125.76 MHz, THF-d_8): δ 149.83 (s, C(5/20)); 134.79 (s, C(6/21)); 123.79 (s, C(11/26)); 117.94 (d, $^1J_{CH}$ = 147.8 Hz, C(10/25)); 117.39 (d, $^1J_{CH}$ = 146.8 Hz, C(9/24)); 111.76

(s, C(8/23)); 110.20 (d, $^1J_{CH}$ = 158.0 Hz, C(3/18)); 102.89 (d, $^1J_{CH}$ = 160.2 Hz, C(4/19)); 67.40 (m, THF); 44.91 (d, $^1J_{CH}$ = 129.4 Hz, C(7/22)); 37.96 (d, $^1J_{CH}$ = 127.7 Hz, C(13/28)); 25.45 (m, THF); 24.53, 21.69 (2q, $^1J_{CH}$ = 125.5 Hz, 124.5 Hz, C(14/15/29/30)); 24.33 (q, $^1J_{CH}$ = 124.8 Hz, C(12/27); 12.61 (q, $^1J_{CH}$ = 124.3 Hz, C(1/16)).

The proton and carbon signals in the NMR spectra of **2** are labeled according to the numbering scheme shown in the following figure.
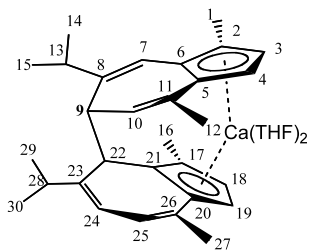
4.1.2. ^1H-NMR data for 2

^{1}H-NMR (500.13 MHz, THF-d_8): δ 6.12 (s, 1H, H(7)); 5.67 (d, $^3J_{HH}$ = 3.30 Hz, 1H, H(19)); 5.62 (d, $^3J_{HH}$ = 3.30 Hz, 1H, H(18)); 5.46 (s, 2H, H(24)+H(25)); 5.44 (s, 2H, H(3)+H(4)); 5.21 (dd, $^3J_{HH}$ = 8.58 Hz, $^3J_{HH}$ = 1.13 Hz, 1H, H(10)); 3.39 (d, $^3J_{HH}$ = 2.0 Hz, 1H, H(22)); 3.07 (dd, $^3J_{HH}$ = 8.58 Hz, $^3J_{HH}$ = 2.0 Hz, 1H, H(9)); 2.52 (hept, $^3J_{HH}$ = 6.71 Hz, 1H, H(28)); 2.45 (hept, $^3J_{HH}$ = 6.71 Hz, 1H, H(13)); 1.96 (s, 3H, H(1)); 1.93 (s, 3H, H(16)); 1.90 (s, 3H, H(12)); 1.80 (s, 3H, H(27)); 1.25, 1.13 (2d, $^3J_{HH}$ = 6.71(3H), 6.71 Hz(3H), H(14)+H(15)); 1.08, 0.93 (2d, $^3J_{HH}$ = 6.71 (3H), 6.71 Hz (3H), H(29)+H(30)). ^{13}C-NMR (125.77 MHz, THF-d_8): δ 144.86 (s, C(20)); 136.99 (s, C(6)); 134.64 (s, C(21)); 130.44 (s, C(5)); 125.24 (s, C(17)); 122.46 (s, C(26)); 121.81 (s, C(11)); 119.37 (d, $^1J_{CH}$ = 144.2 Hz, C(25)); 119.14 (s, C(23)); 118.54 (d, $^1J_{CH}$ = 149.9 Hz, C(24)); 118.05 (d, $^1J_{CH}$ = 151.7 Hz, C(10)); 116.46 (d, $^1J_{CH}$ = 143.5 Hz, C(7)); 116.10 (s, C(8)); 113.54 (s, C(2)); 109.10 (d, $^1J_{CH}$ = 158.0 Hz, C(18)); 106.85 (d, $^1J_{CH}$ = 159.0 Hz, C(3)); 105.70 (d, $^1J_{CH}$ = 160.0 Hz, C(4)); 103.53 (d, $^1J_{CH}$ = 159.6 Hz, C(19)); 52.02 (d, $^1J_{CH}$ = 122.4 Hz, C(9)); 48.62 (d, $^1J_{CH}$ = 121.4 Hz, C(22)); 37.14 (d, $^1J_{CH}$ = 125.2 Hz, C(28)); 36.39 (d, $^1J_{CH}$ = 123.5 Hz, C(13)); 25.01 (q, $^1J_{CH}$ = 122.1 Hz, C(16)); 24.95 (q, $^1J_{CH}$ = 124.7 Hz, C(14/15)); 24.45 (q, $^1J_{CH}$ = 124.8 Hz, C(27)); 24.27 (q, $^1J_{CH}$ = 125.3 Hz, C(29/30)); 22.29 (q, $^1J_{CH}$ = 124.6 Hz, C(29/30)); 22.16 (q, $^1J_{CH}$ = 124.3 Hz, C(14/15)); 13.91 (q, $^1J_{CH}$ = 124.1 Hz, C(1)); 13.40 (q, $^1J_{CH}$ = 123.7 Hz, C(12)).

4.2. Thermolyses of 1 and 2

A solution of 43 mg (0.081 mmol) of **2DME** in 0.4 mL of THF-d_8 was sealed in an NMR tube and heated in an oil bath at 85–90 °C. ^{1}H-NMR spectra were taken at regular intervals. The NMR spectra showed that the resonances of **1** increased while the resonances of isomer **2** decreased. After 36 h, none of isomer **2** remained. A ^{1}H-NMR spectrum showed the presence of complex **1** (90%) and free guaiazulene (8%). Heating of a solution of 52 mg (0.090 mmol) of **1** in 0.45 ml of THF-d_8 was performed under the same conditions. No formation of isomer **2** was observed. A ^{1}H-NMR spectrum revealed free guaiazulene (2–3%) indicating that some decomposition had occurred.

4.3. X-ray structure determination

Crystals of compound **1** were covered with a layer of hydrocarbon oil, and a suitable crystal was selected and attached to a glass fiber using grease. Data for the crystal was collected at 203(2) K using a Bruker/Siemens SMART 1K instrument equipped with a LT-2A low temperature device. Data were measured using omega scans of 0.3° per frame for 5 s. A half sphere of data was collected giving a total of 1471 frames with a final resolution of 0.84 Å. The first 50 frames were recollected at the end of each data collection to monitor for decay. Cell parameters were retrieved using SMART [15] software and refined using SAINTPLUS [16] on all observed reflections. Data reduction and correction for Lp and decay were performed using the SAINTPLUS software. Absorption corrections were applied using SADABS [17]. The structure was solved by direct methods and refined by least-squares method on F^2 using the SHELXTL program package [18]. The structure was solved in the space group $P2_1/c$ (#14) by analysis of systematic absences. All non-hydrogen atoms were refined anisotropically. Hydrogen atoms were added geometrically and refined with a riding model with their parameters constrained to the parent atom site. There is a 0.5 occupied THF molecule in the formula unit. No decomposition was observed during data collection.

5. Supplementary material

Acknowledgements

References

[1] (a) H. Schwemlein, H.H. Brintzinger, J. Organomet. Chem. 254 (1983) 69;
(b) S. Guttmann, P. Burger, H.U. Hund, J. Hofmann, H.H. Brintzinger, J. Organomet. Chem. 369 (1989) 343.

[2] (a) M. Rieckhoff, U. Pieper, D. Stalke, F.T. Edelmann, Angew. Chem. Int. Ed. Engl. 32 (1993) 1079;
(b) K.M. Kane, P.J. Shapiro, R. Cubbon, A. Vij, A.L. Rheingold, Organometallics 16 (1997) 4567;
(c) M. Könemann, G. Erker, R. Fröhlich, S. Kotila, Organometallics 16 (1997) 2900;
(d) G.J. Matare, K.M. Kane, P.J. Shapiro, A. Vij, J. Chem. Cryst. 28 (1998) 731;
(e) P.J. Shapiro, K.M. Kane, A. Vij, D. Stelck, G.J. Matare, R.L. Hubbard, B. Caron, Organometallics 18 (1999) 3468;
(f) G.J. Matare, D.M.J. Foo, K.M. Kane, R. Zehnder, M. Wagener, P.J. Shapiro, T. Concolino, A.L. Rheingold, Organometallics 19 (2000) 1534;
(g) B. Twamley, G.J. Matare, P.J. Shapiro, A. Vij, Acta Crystallogr. E57 (2001) m402;
(h) B. Höhn, P.-J. Sinnema, R.L. Hubbard, P.J. Shapiro, B. Twamley, A. Vij, Organometallics 21 (2002) 182.

[3] (a) A. Recknagel, F.T. Edelmann, Angew. Chem. Int. Ed. Engl. 30 (1991) 693;
(b) F.T. Edelmann, M. Rieckhoff, I. Haiduc, I. Silaghi-Dumitresco, J. Organomet. Chem. 447 (1993) 203;
(c) I.L. Fedushkin, S. Dechert, H. Schumann, Angew. Chem. Int. Ed. 40 (2001) 561.

[4] J.J. Eisch, X. Shi, F.A. Owuor, Organometallics 17 (1998) 5219.

[5] (a) T.S. Tan, J.L. Fletcher, M.J. McGlinchey, J. Chem. Soc Chem. Commun. (1975) 771;
(b) R. Teuber, R. Köppe, G. Linti, M. Tacke, J. Organomet. Chem. 545–546 (1997) 105;
(c) J.A. Bandy, V.S.B. Mtetwa, K. Prout, J. Chem. Soc. Dalton Trans. (1985) 2037.

[6] P. Burger, H.U. Hund, K. Evertz, H.H. Brintzinger, J. Organomet. Chem. 378 (1989) 153.

[7] M. Könemann, G. Erker, R. Fröhlich, S. Kotila, Organometallics 16 (1997) 2900.

[8] Recently the structure of *rac*-(3,3′-diacenaphthylenide)calcium bis(tetrahydrofuran) adduct was established: P.-J. Sinnema, B. Twamley, P.J. Shapiro, Acta Crystallogr. E57 (2001) m438.

[9] I.L. Fedushkin, T.V. Petovskaya, M.N. Bochkarev, S. Dechert, H. Schumann, Angew. Chem. Int. Ed. 40 (2001) 2474.

[10] Piet-Jan Sinnema, unreported results.

[11] The formula and the unit cell for **2** were determined at 203(2) K: $C_{34}H_{46}CaO_2$, (one DME molecule coordinated to the central calcium); Monoclinic, $P2_1/c$; $a = 11.508(6)$, $b = 32.809(18)$, $c = 16.440(9)$, $b = 101.62(1)$, $V = 6080(6)$.

[12] In general, dissolving of calcocene DME adducts in THF-d_8 results in replacement of DME by THF. In this case, consequently, the NMR spectrum will be that of [8,6′-diguaiazulenide]Ca(THF)$_2$.

[13] Fischer et al. reported first on bis(azulene)iron, the molecular structure of which was established by Churchill and coworkers. See: (a) E.O. Fischer, J. Müller, J. Organomet. Chem. 1 (1964) 464. (b) M.R. Churchill, J. Wormald, J. Chem. Soc. Chem. Commun. (1968) 1033. (c) M.R. Churchill, J. Wormald, Inorg. Chem. 8 (1969) 716.

[14] It is possible that the alternate isomers were produced in the earlier cases and not detected, especially since yields of 8,8′-(diguaiazulenide)titanium dichloride(10%) and 6,8′-(diazulenide)iron (5%) were quite low. A referee has also noted that the differences in stereoselectivity observed among the three cases may be associated with both: (a) differences in the size of the metal involved in the fulvene coupling (Ca vs. Mg) and (b) differences in the amount of covalency in the bonding between the metal and the ligand (s-block metals vs. d-block metal).

[15] SMART v.5.025, Bruker Molecular Analysis Research Tool, Bruker AXS, Madison, WI, 1998.

[16] SAINTPLUS v. 6.02, Data Reduction and Correction Program, Bruker AXS, Madison, WI, 1998.

[17] G.M Sheldrick, SADABS v.2.01, an empirical absorption correction program, Bruker AXS, Madison, WI, 1999.

[18] G.M. Sheldrick, SHELXTL v. 5.10, Structure Determination Software Suite, Bruker AXS, Madison, WI, 1997–1998.